PHYSICAL REVIEW D **94,** 105013 (2016)

Instanton-dyon liquid model. V. Twisted light quarks

Yizhuang Liu,[*] Edward Shuryak,[†] and Ismail Zahed[‡]

Department of Physics and Astronomy, Stony Brook University, Stony Brook, New York 11794-3800, USA

(Received 21 June 2016; published 14 November 2016)

We discuss an extension of the instanton-dyon liquid model that includes twisted light quarks in the fundamental representation with explicit Z_{N_c} symmetry for the case with an equal number of colors N_c and flavors N_f. We map the model on a three-dimensional quantum effective theory, and analyze it in the mean-field approximation. The effective potential and the vacuum chiral condensates are made explicit for $N_f = N_c = 2,\ 3$. The low temperature phase is center symmetric but breaks spontaneously flavor symmetry with $N_f - 1$ massless pions. The high temperature phase breaks center symmetry but supports finite and unequal quark condensates.

DOI: 10.1103/PhysRevD.94.105013

I. INTRODUCTION

In the QCD ground state confinement and chiral symmetry breaking are intertwined as lattice simulations have now established [1]. The loss of confinement with increasing temperature as described by a jump in the Polyakov line is followed by a rapid crossover in the chiral condensate for $2+1$ flavors. When the quarks are in the adjoint representation, the crossover occurs much later than the deconfinement transition. There is increasing lattice evidence that the topological nature of the underlying gauge configurations may be key in understanding some aspects of these results [2].

This work is a continuation of our earlier studies [3–6] of the gauge topology using the instanton-dyon liquid model. The starting point of the model is the Kraan-van-Ball-Lee-Lu (KvBLL) instantons threaded by finite holonomies and their splitting into instanton-dyon constituents [7], with strong semiclassical interactions [8–10]. At low temperature, the phase preserves center symmetry but breaks spontaneously chiral symmetry. At sufficiently high temperature, the phase restores both symmetries as the constituent instanton-dyons regroup into topologically neutral instanton-anti-instanton molecules. The importance of fractional topological constituents for confinement was initially suggested through instanton-quarks in [11], and more recently using bions in [12].

The instanton-dyons carry fractional topological charge $1/N_c$ and are able to localize chiral quarks into zero modes. For quarks in the fundamental representation, as the KvBLL instanton fractionates, the zero mode migrates to the heavier instanton-dyon constituent [13]. The random hopping of these zero modes in the instanton-dyon liquid is at the origin of the spontaneous breaking of chiral symmetry as has been shown both numerically [14,15] and using mean-field methods [4]. In supersymmetric QCD some arguments were presented in [16].

At finite temperature the light quarks are subject to antiperiodic boundary conditions on S^1 to develop the correct occupation statistics in bulk. General twisted fermionic boundary conditions on S^1 amount to thermal QCD with Bohm-Aharanov phases that alter fundamentally the nature of the light quarks [17,18]. A particularly interesting proposal consists of a class of Z_{N_c} twisted QCD boundary conditions with $N_c = N_f$, resulting in a manifestly Z_{N_c} symmetric QCD dubbed Z_{N_c}-QCD [19]. The confined phase is both center and chiral symmetric even though the boundary conditions are flavor breaking. The deconfined phase is center and chiral symmetry broken [19,20].

The purpose of this paper is to address some aspects of twisted fermionic boundary conditions in the context of the instanton-dyon liquid model. Since the localization of the zero modes on a given instanton species is very sensitive to the nature of the twist on S^1, this deformation offers an insightful tool for the possible understanding of the fundamental aspects of the spontaneous breaking of chiral symmetry through the underlying topological constituents. Similar issues were addressed using Polyakov-Nambu-Jona-Lasinio (PNJL) models [19] and more recently monopole-dyons and without antimonopole-dyons for small S^1 [21]. A numerical analysis in the instanton-dyon liquid model with $N_f = N_c = 2$ was recently presented in [22].

In Sec. II we briefly review the model and discuss the general case of $N_c = N_f$ twisted boundary conditions. The special cases of $N_c = N_f = 2,\ 3$ are given and the corresponding normalizable zero modes around the center symmetric point constructed. We derive explicitly the pertinent hopping matrices between the instanton-dyons and the instanton-antidyons for the case of $N_c = N_f = 2, 3$ which are central to the quantitative study of the spontaneous breaking of chiral symmetry. In Sec. III we use a series of fermionization and bosonization transformations

[*]yizhuang.liu@stonybrook.edu
[†]edward.shuryak@stonybrook.edu
[‡]ismail.zahed@stonybrook.edu

to map the instanton-dyon partition function on a three-dimensional effective theory. For $N_f > 2$, additional discrete symmetries combining charge conjugation and exchange between conjugate flavor pairs are identified, with the same chiral condensates at high temperature. In Sec. IV we derive the effective potential for the ground state of the three-dimensional effective theory. We explicitly show that it supports a center symmetric state with spontaneously broken chiral symmetry. The center asymmetric phase at high temperature supports unequal chiral condensates. Our conclusions are in Sec. V.

II. EFFECTIVE ACTION WITH TWISTED FERMIONS

A. General setting

For simplicity we detail here the general setting for $N_c = 2$. The pertinent changes for any N_c will be quoted when appropriate. For a fixed holonomy with $A_4(\infty)/2\omega_0 = \nu\tau^3/2$ and $\omega_0 = \pi T$, the SU(2) KvBLL instanton [7] is composed of a pair of instanton-dyons labeled by L, M (instanton-antidyons by $\overline{\rm L}, \overline{\rm M}$). In general, there are $N_c - 1$ BPS instanton-dyons and only one twisted instanton-dyon. As a result the global gauge symmetry is reduced through $SU(N_c) \to U(1)^{N_c-1}$.

For example, the grand-partition function for dissociated $N_c = 2$ KvBLL instantons and anti-instantons and N_f massless flavors is

$$\mathcal{Z}_1[T] \equiv \sum_{[K]} \prod_{i_L=1}^{K_L} \prod_{i_M=1}^{K_M} \prod_{i_{\overline{L}}=1}^{K_{\overline{L}}} \prod_{i_{\overline{M}}=1}^{K_{\overline{M}}} \times \int \frac{f_L d^3x_{Li_L}}{K_L!} \frac{f_M d^3x_{Mi_M}}{K_M!} \frac{f_L d^3y_{\overline{L}i_{\overline{L}}}}{K_{\overline{L}}!} \frac{f_M d^3y_{\overline{M}i_{\overline{M}}}}{K_{\overline{M}}!} \times \det(G[x])\det(G[y])|\det\tilde{\mathbf{T}}(x,y)|^{N_f} e^{-V_{D\overline{D}}(x-y)}. \quad (1)$$

Here x_{mi} and y_{nj} are the three-dimensional coordinates of the i-dyon of m-kind and j-antidyon of n-kind. Here $G[x]$ is a $(K_L + K_M)^2$ matrix and $G[y]$ a $(K_{\overline{L}} + K_{\overline{M}})^2$ matrix whose explicit forms are given in [8,9]. $V_{D\overline{D}}$ is the streamline interaction between $\mathrm{D} = \mathrm{L}, \mathrm{M}$ dyons and $\overline{\mathrm{D}} = \overline{\mathrm{L}}, \overline{\mathrm{M}}$ antidyons as numerically discussed in [10]. For the SU(2) case it is Coulombic asymptotically with a core at short distances [3]. We will follow our original discussion with light quarks in [4], with the determinantal interactions in (1) providing for an effective core repulsion on average. We omit the explicit repulsion between the cores as in [6], for simplicity. The fugacities f_i are related to the overall instanton-dyon density, and can be estimated using lattice simulations [2]. Here they are external parameters, with a dimensionless density

$$\mathbf{n} = \frac{4\pi\sqrt{f_L f_M}}{\omega_0^2} \approx \mathbf{C} e^{-\frac{S(T)}{2}}. \quad (2)$$

For definiteness, the KvBLL instanton action to one loop is

$$S(T) \equiv \frac{2\pi}{\alpha_s(T)} = \left(11\frac{N_c}{3} - 2\frac{N_f}{3}\right)\ln\left(\frac{T}{0.36T_D}\right). \quad (3)$$

The fermionic determinant $\det\tilde{\mathbf{T}}(x,y)$ with twisted quarks will be detailed below. In many ways (1) resembles the partition function for the instanton-anti-instanton ensemble [23].

B. Twisted boundary conditions and normalizable zero modes

Consider $N_f = N_c$ QCD on $S^1 \times R^3$ with the following antiperiodic boundary conditions modulo a flavor twist in the center of $SU(N_c)$,

$$\psi_f(\beta, \vec{x}) = -z^{f-1}\psi_f(0, \vec{x}), \quad (4)$$

with $z = e^{i2\pi/N_c}$ and $f = 1, 2, 3, \ldots = u, d, s, \ldots$ respectively. Under a Z_{N_c} twisted gauge transformation of the type

$$\Omega(\beta, \vec{x}) = z^k \Omega(0, \vec{x}), \quad (5)$$

(4) is $Z_{N_c+N_f}$ symmetric following the flavor relabeling $f + k \to f$. As a result the theory is usually referred to as Z_{N_c}-QCD [19]. In contrast, (4) breaks explicitly chiral flavor symmetry through

$$U_L(N_f) \times U_R(N_f) \to U_L^{N_f}(1) \times U_R^{N_f}(1). \quad (6)$$

To construct explicitly the fermionic zero modes in a Bogomolny-Prasad-Sommerfeld (BPS) or KK dyon with the twisted boundary conditions (4), we consider the generic boundary condition

$$\psi(x_4 + \beta, \vec{x}) = -e^{i\phi}\psi(x_4, \vec{x}) \quad (7)$$

and redefine the quark field through $\psi = e^{iT\phi x_4}\tilde{\psi}$. The latter satisfies a modified Dirac equation with an imaginary chemical potential $-\phi T$ [17],

$$(i\gamma \cdot D - \gamma_4 T\phi)\tilde{\psi} = 0. \quad (8)$$

In a BPS dyon with periodic boundary conditions, the solution to (8) asymptotes

$$\tilde{\psi} \to e^{-\pi T\nu r \pm \phi T r} \quad (9)$$

which is normalizable for $|\phi| < \pi\nu$. For the antiperiodic boundary condition, the requirement for the existence of a normalizable zero mode in a BPS dyon is $|\phi - \pi| < \pi\nu$.

C. Case: $N_c = N_f = 3$

For $N_c = N_f = 3$, the flavor twisted boundary condition (4) takes the explicit form

$$\begin{aligned} u(\beta) &= -u(0) \\ d(\beta) &= e^{-i\pi/3} d(0) \\ s(\beta) &= e^{+i\pi/3} s(0). \end{aligned} \tag{10}$$

The d,s boundary conditions in (10) admit a discrete symmetry under the combined charge conjugation and the flavor exchange $d \leftrightarrow s$.

The normalizability condition for the quark zero modes following from the flavor twisted boundary conditions in (8)–(9) shows that $f = 1 = u$ always supports a normalizable KK zero mode, while $f = 2, 3 = d, s$ supports BPS zero modes that are at the edge of the normalizability domain in the symmetric phase with $\nu = 1/3$. The BPS modes carry a time dependence of the form $e^{\pm\frac{i\omega_0}{3}x_4}$ as $\nu \to 1/3$, while the KK mode carries a time dependence of the form $e^{i\omega_0 x_4}$. In both cases, we are restricting the modes to the lowest frequencies in Euclidean x_4-time, for simplicity. This means a moderately large temperature ranging from the center symmetric to asymmetric phase.

The explicit form of the twisted zero modes in a BPS dyon and satisfying the twisted boundary condition (7) can be obtained in closed form in the hedgehog gauge,

$$\tilde{\psi}_{\mp,A\alpha}(r) = (\alpha_1(r)\epsilon + \alpha_2(r)\sigma\cdot\hat{r}\epsilon)_{A\alpha} \tag{11}$$

in color-spin, with $\epsilon_{A\alpha} = -\epsilon_{\alpha A}$ and

$$\begin{aligned} \alpha_{1,2}(r) &= \frac{\chi_{1,2}(r)}{\sqrt{2\pi\nu T r \sinh(2\pi\nu \mathrm{Tr})}} \\ \chi_1(r) &= -\frac{\tilde{\phi}}{\pi\nu}\sinh(\tilde{\phi}\mathrm{Tr}) + \tanh(\pi T\nu r)\cosh(\tilde{\phi}\mathrm{Tr}) \\ \chi_2(r) &= \mp\left(\frac{\tilde{\phi}}{\pi\nu}\cosh(\tilde{\phi}\mathrm{Tr}) - \coth(\pi T\nu r)\sinh(\tilde{\phi}\mathrm{Tr})\right). \end{aligned} \tag{12}$$

Here $\tilde{\phi} \equiv \phi - \pi$ and $\mp$ refers to M, $\overline{M}$ respectively. Asymptotically, the BPS zero modes take the compact form in the hedgehog gauge

$$\begin{aligned} (\tilde{\psi}_M\epsilon)(r) &\to \frac{1 + \mathrm{sgn}(\tilde{\phi})\sigma\cdot\hat{r}}{\sqrt{2\pi T\nu r \sinh(2\pi T\nu r)}} e^{|\tilde{\phi}|Tr} \\ (\tilde{\psi}_{\overline{M}}\epsilon)(r) &\to \frac{1 - \mathrm{sgn}(\tilde{\phi})\sigma\cdot\hat{r}}{\sqrt{2\pi T\nu r \sinh(2\pi T\nu r)}} e^{|\tilde{\phi}|Tr}. \end{aligned} \tag{13}$$

For the KK instanton-dyon, we recall the additional time-dependent gauge transformation from the BPS instanton-dyon. The explicit forms of the zero modes are also similar (11)–(13) with now $\tilde{\phi} = \phi$. We note that for the flavor twisted boundary condition (4), $f = d$, s corresponds to $\tilde{\phi} = \mp\pi/3 \pmod{2\pi}$ in (13) which are not normalizable BPS zero modes at exactly $\nu = 1/3$. Following our analysis in [6], we choose to regulate the zero modes by approaching the holonomies in the center symmetric phase as follows ($\epsilon_{1,2} \to +0$):

$$\begin{aligned} \nu_{M1} &= \frac{1}{3} + \epsilon_1 \\ \nu_{M2} &= \frac{1}{3} - \epsilon_2 \\ \nu_L &= \frac{1}{3} + \epsilon_2 - \epsilon_1. \end{aligned} \tag{14}$$

As a result, the M1-instanton-dyon carries two zero modes (d,s); the M2-instanton-dyon carries none; and the L-dyon carries one zero mode (u). This regularization enforces the Nye-Singer index theorem for fundamental quarks [24] and the discrete symmetry noted earlier.

D. Case: $N_c = N_f = 2$

For the case of $N_f = N_c = 2$, a more general set of twisted boundary conditions will be analyzed with

$$\begin{aligned} u(\beta) &= e^{i\theta}(-u(0)) \\ d(\beta) &= e^{i\theta}(-e^{i\pi}d(0)) \end{aligned} \tag{15}$$

which is (4) for $\theta = 0$. (15) is seen to have the additional discrete symmetry when $\theta \to \pi - \theta$ and $u \leftrightarrow d$ at $\nu = 1/2$. Thus, only the range $\theta < \pi/2$ will be considered. In this case, the M-instanton-dyon carries one zero mode (d), while the L-instanton-dyon carries one zero mode (u). For (15) the normalizable zero modes are asymptotically of the form (13) with $\phi = \theta$.

For completeness we note the Roberge-Weiss boundary condition [17]

$$\begin{aligned} u(\beta) &= e^{i\theta}u(0) \\ d(\beta) &= e^{i\theta}d(0). \end{aligned} \tag{16}$$

In the range $0 < \theta < \pi/2$, the M-instanton-dyon carries two zero modes with none on the L-instanton-dyon. In the range $\frac{\pi}{2} < \theta < \frac{3\pi}{2}$, the two zero modes jump onto the L-instanton-dyon. In the range $0 < \frac{3\pi}{2} < \theta < 2\pi$ they jump back on the M-instanton-dyon. We note that for $\theta = \theta_0 + \pi/2$ with $0 < \theta_0 < \pi/2$, the M-zero mode moves to be an L-zero mode with the asymptotic

$$\frac{(1 - \sigma\cdot\hat{r})}{\sqrt{r\sinh(\pi\mathrm{Tr})}} e^{(\pi/2-\theta_0)Tr} e^{i(\theta_0-\pi/2)Tx_4} e^{i\pi Tx_4}. \tag{17}$$

This is to be compared to the case with $\theta = \frac{\pi}{2} - \theta_0$ with the asymptotic

$$\frac{(1+\sigma\cdot\hat{r})}{\sqrt{r\sinh(\pi \mathrm{T} r)}} e^{(\pi/2-\theta_0)Tr} e^{i(\frac{\pi}{2}-\theta_0)Tx_4}. \tag{18}$$

E. Twisted fermionic determinant

The fermionic determinant can be viewed as a sum of closed fermionic loops connecting all instanton-dyons and instanton-antidyons. Each link—or hopping—between an instanton-dyon and $\overline{\mathrm{L}}$-anti-instanton-dyon is described by the hopping chiral matrix

$$\tilde{\mathbf{T}}(x,y) \equiv \begin{pmatrix} 0 & i\mathbf{T}_{ij} \\ i\mathbf{T}_{ji} & 0 \end{pmatrix}. \tag{19}$$

Each of the entries in $\mathbf{T}_{ij}$ is a "hopping amplitude" of a fermionic zero mode φ_D from an instanton-dyon to a zero mode $\varphi_{\overline{D}}$ (of opposite chirality) of an instanton-antidyon:

$$\begin{aligned} \mathbf{T}_{LR}(x_{LR}) &= \int d^4x \varphi_L^\dagger(x-x_L) i(\partial_4 - i\sigma\cdot\nabla)\varphi_R(x-x_R) \\ \mathbf{T}_{RL}(x_{LR}) &= \int d^4x \varphi_R^\dagger(x-x_L) i(\partial_4 + i\sigma\cdot\nabla)\varphi_L(x-x_R) \end{aligned} \tag{20}$$

with $x_{LR} \equiv x_L - x_R$, and similarly for the other components. In the hedgehog gauge, these matrix elements can be made explicit in momentum space. Their Fourier transform is

$$T_{LR}(p) = \mathrm{Tr}(\varphi_L^\dagger(p)(-\Phi T - i\sigma\cdot p)\varphi_R(p)) \tag{21}$$

with ΦT the contribution from the lowest Matsubara mode retained. We recall that the use of the zero modes in the string gauge to assess the hopping matrix elements introduces only minor changes in the overall estimates as we discussed in [4] (see Appendix A).

1. Case $N_c = N_f = 3$

For general ν, we use the Fourier transform of the zero modes (11) in (21) to obtain

$$T_i(p) = \Phi_i T(F_{2i}^2(p) - F_{1i}^2(p)) + \mathrm{sgn}(\tilde{\phi}_i) 2pF_{1i}(p)F_{2i}(p). \tag{22}$$

The key physics in the Fourier transforms $F_{1,2}(p)$ is captured by retaining only the flux-induced masslike contribution in the otherwise massless asymptotics, i.e.

$$F_{1i}(p) \approx \frac{1}{3}F_{2i}(p) \approx \frac{\omega_0}{(p^2 + ((\nu - |\tilde{\phi}_i|/\pi)\omega_0)^2)^{\frac{5}{4}}}. \tag{23}$$

The i-assignments are respectively given by

$$i \equiv (\overline{L}L, \overline{M}_1 M_1, \overline{M}_2 M_2) \qquad \begin{cases} \tilde{\phi}_i = (0, -\frac{\pi}{3}, +\frac{\pi}{3}) \\ \Phi_i = (\pi, -\frac{\pi}{3}, +\frac{\pi}{3}) \end{cases}. \tag{24}$$

In the center symmetric phase with $\nu = 1/3$, (22) is long-ranged for the M-instanton-dyons,

$$T_3(p) = -T_2(p) \approx \Phi T \frac{8C^2}{p^5} + \mathrm{sgn}(\tilde{\phi}) \frac{6C^2}{p^4}. \tag{25}$$

Here C is a normalization constant fixed by the regularization detailed in (14).

2. Case $N_c = N_f = 2$

For $N_c = N_f = 2$, the Fourier transform of the lowest Matsubara zero mode for both boundaries (15)–(16) is

$$\psi_M(p) = f_1(p) - i\mathrm{sgn}(\theta) f_2(p) \sigma\cdot\hat{p}. \tag{26}$$

The corresponding hopping matrix is $(0 \le \theta < \pi/2)$

$$T_{LR}(p) = \tilde{\theta} T(f_2^2(p) - f_1^2(p)) + \mathrm{sgn}(\theta) 2p f_1(p) f_2(p) \tag{27}$$

with the assignments

$$\tilde{\theta} = \begin{cases} \theta - \pi : u \\ \theta : d \end{cases}. \tag{28}$$

and

$$f_1(p) \approx \frac{1}{3} f_2(p) \approx \frac{\omega_0}{(p^2 + ((\nu_i - \theta/\pi)\omega_0)^2)^{\frac{5}{4}}}. \tag{29}$$

It follows that

$$T_{LR}(p) \approx f_1(p)^2 (8\tilde{\theta} T + 6\mathrm{sgn}(\theta) p). \tag{30}$$

Using (17)–(18) we note that the hopping matrix element (30) satisfies the antiperiodicity condition

$$T_{LR}(p, \theta_0 + \pi/2) = -T_{LR}(p, \theta_0 - \pi/2) \tag{31}$$

with the θ-argument exhibited for clarity.

III. $SU(N_c)$ ENSEMBLE

Following [3,4,8] the moduli determinants in (1) can be fermionized using $2N_c$ pairs of ghost fields $\chi_m, \chi_m^\dagger$ for the instanton-dyons and $2N_c$ for the instanton-antidyons. The ensuing Coulomb factors from the determinants are then bosonized using $2N_c$ boson fields v_m, w_m for the instanton-dyons and similarly for the instanton-antidyons. The result is

$$S_{1F}[\chi,v,w]=-\frac{T}{4\pi}\int d^3x \times\sum_{m=1}^{N_c}(|\nabla\chi_m|^2+\nabla v_m\cdot\nabla w_m) +\sum_{\overline{m}=1}^{N_c}(|\nabla\chi_{\overline{m}}|^2+\nabla v_{\overline{m}}\cdot\nabla w_{\overline{m}}). \quad (32)$$

For the streamline interaction part $V_{D\overline{D}}$, we note that as a pair interaction in (1) between the instanton-dyons and instanton-antidyons, it can be bosonized using standard methods [25,26] in terms of $\vec{\sigma}$ and $\vec{b}$ fields. As a result each dyon species acquires additional fugacity factors of the form

$$M:\ e^{-\vec{\alpha}_i\cdot\vec{b}+i\vec{\alpha}_i\cdot\vec{\sigma}} \qquad \overline{M}:\ e^{-\vec{\alpha}_i\cdot\vec{b}-i\vec{\alpha}_i\cdot\vec{\sigma}} \quad (33)$$

with $\vec{\alpha}_i$ and $i=1,2,\ldots N_c-1$ the ith root of the $SU(N_c)$ Lie generator, and $i=N_c$ its affine root due to its compactedness. Therefore, there is an additional contribution to the free part (32)

$$S_{2F}[\sigma,b]=\frac{T}{8}\int d^3x(\nabla\vec{b}\cdot\nabla\vec{b}+\nabla\vec{\sigma}\cdot\nabla\vec{\sigma}) \quad (34)$$

where for simplicity we approximated the streamline by a Coulomb interaction, and the interaction part is now

$$\begin{aligned}S_I[v,w,b,\sigma,\chi] &= -\int d^3x\Bigg(\sum_{i=1}^{N_c}e^{-\vec{\alpha}_i\cdot\vec{b}+i\vec{\alpha}_i\cdot\vec{\sigma}}f_i \times(4\pi v_i+|\chi_i-\chi_{i+1}|^2+v_i-v_{i+1})e^{w_i-w_{i+1}} \\ &+\sum_{\overline{i}=1}^{N_c}e^{-\vec{\alpha}_{\overline{i}}\cdot\vec{b}-i\vec{\alpha}_{\overline{i}}\cdot\vec{\sigma}}f_{\overline{i}} \times(4\pi v_i+|\chi_{\overline{i}}-\chi_{\overline{i}+1}|^2+v_{\overline{i}}-v_{\overline{i}+1})e^{w_{\overline{i}}-w_{\overline{i}+1}}\Bigg) \end{aligned} \quad (35)$$

without the fermions. We now show the minimal modifications to (35) when the fermionic determinantal interaction is included.

A. Fermionic fields

To fermionize the determinant in (1) and for simplicity, consider first the case of $N_f=1$ fermionic zero modes attached to the kth instanton-dyon, and define the additional Grassmanians $\chi=(\chi_1^i,\chi_2^j)^T$ with $i,j=1,..,K_{k,\overline{k}}$ so that

$$|\det\tilde{\mathbf{T}}|=\int D[\chi]e^{\chi^\dagger\tilde{\mathbf{T}}\chi}. \quad (36)$$

We can rearrange the exponent in (36) by defining a Grassmanian source $J(x)=(J_1(x),J_2(x))^T$ with

$$J_1(x)=\sum_{i=1}^{K_L}\chi_1^i\delta^3(x-x_{ki}) \qquad J_2(x)=\sum_{j=1}^{K_{\overline{L}}}\chi_2^j\delta^3(x-y_{\overline{k}j}) \quad (37)$$

and by introducing two additional fermionic fields $\psi_k(x)=(\psi_{k1}(x),\psi_{k2}(x))^T$. Thus

$$e^{\chi^\dagger\tilde{\mathbf{T}}\chi}=\frac{\int D[\psi]\exp(-\int\psi_k^\dagger\tilde{\mathbf{G}}\psi_k+\int J^\dagger\psi_k+\int\psi_k^\dagger J)}{\int dD[\psi]\exp(-\int\psi_k^\dagger\tilde{\mathbf{G}}\psi_k)} \quad (38)$$

with $\tilde{\mathbf{G}}$ a 2×2 chiral block matrix

$$\tilde{\mathbf{G}}=\begin{pmatrix}0 & -i\mathbf{G}(x,y)\\ -i\mathbf{G}(x,y) & 0\end{pmatrix} \quad (39)$$

with entries $\mathbf{TG}=\mathbf{1}$. The Grassmanian source contributions in (38) generate a string of independent exponents for the L-instanton-dyons and $\overline{\text{L}}$-instanton-antidyons

$$\prod_{i=1}^{K_k}e^{\chi_1^{i\dagger}\psi_{k1}(x_{ki})+\psi_{k1}^\dagger(x_{ki})\chi_1^i} \times\prod_{j=1}^{K_{\overline{k}}}e^{\chi_2^{j\dagger}\psi_{k2}(y_{\overline{k}j})+\psi_{k2}^\dagger(y_{\overline{k}j})\chi_2^j}. \quad (40)$$

The Grassmanian integration over the χ_i in each factor in (40) is now readily done to yield

$$\prod_i[-\psi_{k1}^\dagger\psi_{k1}(x_{ki})]\prod_j[-\psi_{k2}^\dagger\psi_{k2}(y_{\overline{k}j})] \quad (41)$$

for the k-instanton-dyon and $\overline{\text{k}}$-instanton-antidyon. The net effect of the additional fermionic determinant in (1) is to shift the k-instanton-dyon and $\overline{\text{k}}$-instanton-antidyon fugacities in (35) as follows:

$$\begin{aligned}f_k &\to -f_k\psi_{k1}^\dagger\psi_{k1}\equiv -f_L\psi_k^\dagger\gamma_+\psi_k\\ f_{\overline{k}} &\to -f_{\overline{k}}\psi_{k2}^\dagger\psi_{k2}\equiv -f_{\overline{k}}\psi_k^\dagger\gamma_-\psi_k\end{aligned} \quad (42)$$

where we have now identified the chiralities with $\gamma_\pm=(1\pm\gamma_5)/2$. Note that for the instanton-dyons and instanton-antidyons with no zero mode attached, the fugacities remain unchanged.

B. Resolving the constraints

In terms of (32)–(35) and the substitution (42), the instanton-dyon partition function (1) for finite N_f can be

exactly rewritten as an interacting effective field theory in three dimensions,

$$\mathcal{Z}_1[T] \equiv \int D[\psi]D[\chi]D[v]D[w]D[\sigma]D[b] \times e^{-S_{1F}-S_{2F}-S_l-S_\psi} \tag{43}$$

with the additional chiral fermionic contribution $S_\psi = \psi^\dagger \tilde{\mathbf{G}}\psi$. Since the effective action in (43) is linear in the $v_{M,L,\overline{M},\overline{L}}$, the latter integrate to give the following constraints,

$$-\frac{T}{4\pi}\nabla^2 w_k + f_k e^{\vec{\alpha}_k\cdot(-\vec{b}+i\vec{\sigma})}\prod_f \psi^\dagger_{kf}\gamma_+\psi_{kf}e^{w_k-w_{k+1}} - f_{k-1}e^{\vec{\alpha}_{k-1}\cdot(-\vec{b}+i\vec{\sigma})}\prod_f \psi^\dagger_{k-1f}\gamma_+\psi_{k-1f}e^{w_{k-1}-w_k} = 0, \tag{44}$$

and similarly for the antidyons.

To proceed further the formal classical solutions to the constraint equations or $w[\sigma, b]$ should be inserted back into the three-dimensional effective action. The result is

$$\mathcal{Z}_1[T] = \int D[\psi]D[\sigma]D[b]e^{-S} \tag{45}$$

with the three-dimensional effective action

$$S = S_F[\sigma,b] + \int d^3x \sum_f \psi^\dagger_f \tilde{\mathbf{G}}_f \psi_f + \sum_{k=1}^{N_c} 4\pi f_k v_k \int d^3x \prod_f \psi^\dagger_{kf}\gamma_+\psi_{kf}e^{w_k-w_{k+1}+\vec{\alpha}_k\cdot(-\vec{b}+\vec{i}\sigma)} + \sum_{\overline{k}=1}^{N_c} 4\pi f_{\overline{k}} v_{\overline{k}} \int d^3x \prod_f \psi^\dagger_{\overline{k}f}\gamma_-\psi_{\overline{k}f}e^{w_{\overline{k}}-w_{\overline{k}+1}+\vec{\alpha}_{\overline{k}}\cdot(-\vec{b}+\vec{i}\sigma)}. \tag{46}$$

Here S_F is S_{2F} in (34) plus additional contributions resulting from the $w(\sigma, b)$ solutions to the constraint equations (44) after their insertion back. This procedure for the linearized approximation of the constraint was discussed in [3,4].

For the general case with

$$\tilde{\mathbf{G}}_1 \neq \tilde{\mathbf{G}}_2 \neq \cdots \neq \tilde{\mathbf{G}}_{N_f} \tag{47}$$

these contributions in (46) are only $U_L^{N_f}(1) \times U_R^{N_f}(1)$ symmetric, which is commensurate with (6). The determinantal interactions preserve the individual $U_{L+R}(1_k)$ vector flavor symmetries, but upset the individual $U_{L-R}(1_k)$ axial flavor symmetries. However, the latter induce the shifts

$$\psi^\dagger_{kf}\gamma_\pm\psi_{kf} \to e^{2\xi_k}\psi^\dagger_{kf}\gamma_\pm\psi_{kf} \tag{48}$$

which can be reabsorbed by shifting back the constant magnetic contributions

$$\vec{\alpha}_{\overline{k}}\cdot(-\vec{b}+\vec{i}\sigma) \to \vec{\alpha}_{\overline{k}}\cdot(-\vec{b}+\vec{i}\sigma) - 2\xi_k \tag{49}$$

thanks to the free form in (34). This observation is unaffected by the screening of the magneticlike field, since a constant shift $\vec{b} \to \vec{b} + 2\xi_k$ can always be reset by a field redefinition. This hidden symmetry was noted recently in [21]. We note that this observation holds for the general form of the streamline interaction used in [4] as well, due to its vanishing form in momentum space. From (49) it follows that $\sum_k \xi_k = 0$, so that only the axial flavor singlet $U_{L-R}(1)$ is explicitly broken by the determinantal contributions in (46) as expected in the instanton-dyon-antidyon ensemble. As a result, (46) is explicitly $U(1)_L^{N_f} \times U_R^{N_f}(1)/U_{L-R}(1)$ symmetric.

C. Special cases: $N_c = N_f = 2, 3$

For the case $N_c = N_f = 3$ with the twisted boundary condition (10), the fermionic terms in the effective action (46) are explicitly

$$\begin{aligned}&\psi^\dagger_u\tilde{G}_1\psi_u + \psi^\dagger_d\tilde{G}_2\psi_d + \psi^\dagger_s\tilde{G}_3\psi_s \\ &+ 4\pi f_1\nu_1\psi^\dagger_u\gamma_+\psi_u e^{w_1-w_2} \\ &+ 4\pi f_2\nu_2\psi^\dagger_d\gamma_+\psi_d\psi^\dagger_s\gamma_+\psi_s e^{w_2-w_3} + 4\pi f_3\nu_3 e^{w_3-w_1} \\ &+ 4\pi f_{\overline{1}}\overline{\nu}_1\psi^\dagger_u\gamma_-\psi_u e^{\overline{w}_1-\overline{w}_2} \\ &+ 4\pi f_{\overline{2}}\overline{\nu}_2\psi^\dagger_d\gamma_-\psi_d\psi^\dagger_s\gamma_-\psi_s e^{\overline{w}_2-\overline{w}_3} + 4\pi f_{\overline{3}}\overline{\nu}_3 e^{\overline{w}_3-\overline{w}_1}\end{aligned} \tag{50}$$

following the regularization (14) around the center symmetric point. As noted earlier, (50) is explicitly symmetric under the combined charge conjugation and the flavor exchange $d \leftrightarrow s$ since $\tilde{G}_2 = -\tilde{G}_3 \neq \tilde{G}_1$. With this in mind, (50) is symmetric under $(U_L^3(1) \times U_R^3(1))/U_{L-R}(1)$.

For the case $N_c = N_f = 2$ with the twisted boundary condition (15), the fermionic terms in the effective action (46) are now

$$\begin{aligned}&f_M v_M\psi^\dagger_d\gamma_+\psi_d e^{w_M-w_L} + f_L v_L\psi^\dagger_u\gamma_+\psi_u e^{w_L-w_M} \\ &+ f_{\overline{M}}v_{\overline{M}}\psi^\dagger_d\gamma_-\psi_d e^{w_{\overline{M}}-w_{\overline{L}}} + f_{\overline{L}}v_{\overline{L}}\psi^\dagger_u\gamma_-\psi_u e^{w_{\overline{L}}-w_{\overline{M}}}\end{aligned} \tag{51}$$

while for the Roberge-Weiss boundary condition (16) they are

$$\begin{aligned}&f_M v_M\psi^\dagger_u\gamma_+\psi_u\psi^\dagger_d\gamma_+\psi_d e^{w_M-w_L} + f_L v_L e^{w_L-w_M} \\ &+ f_{\overline{M}}v_{\overline{M}}\psi^\dagger_u\gamma_-\psi_u\psi^\dagger_d\gamma_-\psi_d e^{w_{\overline{M}}-w_{\overline{L}}} + f_{\overline{L}}v_{\overline{L}}e^{w_{\overline{L}}-w_{\overline{M}}}.\end{aligned} \tag{52}$$

IV. EQUILIBRIUM STATE

To analyze the ground state and the fermionic fluctuations we bosonize the fermions in (45)–(46) by introducing the identities

$$\int D[\Sigma_k]\delta(\psi_k^\dagger(x)\psi_k(x)+2\Sigma_k(x))=\mathbf{1} \tag{53}$$

and by reexponentiating them to obtain

$$\mathcal{Z}_1[T]=\int D[\psi]D[\sigma]D[b]D[\vec{\Sigma}]D[\vec{\lambda}]e^{-S-S_C} \tag{54}$$

with

$$-S_C=\int d^3x i\Lambda_k(x)(\psi_f^\dagger(x)\psi_k(x)+2\Sigma_k(x)). \tag{55}$$

The ground state is parity even so that $f_{L,M}=f_{\overline{L},\overline{M}}$. By translational invariance, the ground state corresponds to constant $\sigma, b, \vec{\Sigma}, \vec{\Lambda}$. We will seek the extrema of (54) with finite condensates in the mean-field approximation, i.e.

$$\langle\psi_k^\dagger(x)\psi_l(x)\rangle=-2\delta_{kl}\Sigma_k. \tag{56}$$

With this in mind, the classical solutions to the constraint equations (44) are also constant:

$$\begin{aligned} &f_k\left\langle\prod_f\psi_{kf}^\dagger\gamma_+\psi_{kf}\right\rangle e^{w_k-w_{k+1}}\\ &=f_{k+1}\left\langle\prod_f\psi_{k+1f}^\dagger\gamma_+\psi_{k+1f}\right\rangle e^{w_{k+1}-w_{k+1}} \end{aligned} \tag{57}$$

with

$$\left\langle\prod_f\psi_{kf}^\dagger\gamma_+\psi_{kf}\right\rangle=\prod_f\Sigma_{kf} \tag{58}$$

and similarly for the antidyons. The expectation values in (57)–(58) are carried in (54) in the mean-field approximation through Wick contractions. We now proceed to determine the pressure by imposing the successive constraints (57) only after varying and eliminating the w's.

A. $N_c=N_f=3$ in symmetric phase

In the center-symmetric phase, with all holonomies being equal, $\nu_{1,2,3}=1/3$, the pressure simplifies to

$$\begin{aligned} \mathcal{P}_{uds}-\mathcal{P}_{per}&=8\pi(f_1f_2f_3)^{\frac{1}{3}}(\Sigma_u\Sigma_d\Sigma_s)^{\frac{1}{3}}-2\vec{\Lambda}\cdot\vec{\Sigma}\\ &+\sum_{i=1}^3\int\frac{d^3p}{(2\pi)^3}\ln(1+\Lambda_i^2|T_i|^2(p)) \end{aligned} \tag{59}$$

with the individual fermionic terms being

$$\begin{aligned} \mathcal{P}_i&\equiv\int\frac{d^3p}{(2\pi)^3}\ln(1+\Lambda_i^2|T_i|^2(p))\\ &\equiv\omega_0^3\int\frac{d^3\tilde{p}}{(2\pi)^3}\ln\left(1+\frac{\tilde{\Lambda}_i^2}{\tilde{p}^8}\left(1+\frac{4|\tilde{\phi}_i|}{3\pi\tilde{p}}\right)^2\right). \end{aligned} \tag{60}$$

Here $\tilde{p}=p/\omega_0$ and $\tilde{\Lambda}_i=\Lambda/\omega_0^2$ are dimensionless. From (24), we recall the assignment of quark phases $(\tilde{\phi}_1,\tilde{\phi}_2,\tilde{\phi}_3)=(\pi,-\pi/3,+\pi/3)$, for (u,d,s) respectively. The center symmetric phase breaks spontaneously chiral symmetry, as the gap equations have nonzero solutions. Each of the flavor chiral condensates is found to be

$$\frac{\langle\overline{q}q\rangle_{\tilde{\phi}_i}}{T^3}=2\pi^2\tilde{\Lambda}_i\int\frac{d^3\tilde{p}}{(2\pi)^3}\frac{\frac{5}{3\tilde{p}^5}}{1+\frac{\tilde{\Lambda}_i^2}{\tilde{p}^8}(1+\frac{4|\tilde{\phi}_i|}{3\pi\tilde{p}})^2}. \tag{61}$$

We now note that at asymptotically low temperatures, the $1/p^4$ contribution in the hopping matrix element (25) is dominant.

B. $N_c=N_f=3$ in general asymmetric phase

In the general asymmetric phase the holonomies have values away from the center:

$$\begin{aligned} \nu_1&=\frac{1}{3}+\epsilon_1\\ \nu_2&=\frac{1}{3}-\epsilon_2\\ \nu_3&=1-\nu_1-\nu_2. \end{aligned} \tag{62}$$

Note that in general, the parameters $\epsilon_{1,2}$ are not small. With these choices for the holonomies (62), the u-flavor rides the L-instanton-dyon, and the ds-flavors ride the $M1, M2$-instanton-dyons. For the ds-flavors, the hopping matrix elements between the instanton-dyon and anti-instanton-dyon are given by

$$\begin{aligned} T_d(p)&=-T_s(p)\\ &=\frac{\pi T}{3}(F_2^2(p)-F_1^2(p))+2ipF_1(p)F_2(p) \end{aligned} \tag{63}$$

with

$$F_1(p)\approx\frac{1}{3}F_2(p)\approx\frac{\omega_0}{(p^2+((\nu_1-1/3)\omega_0)^2)^{\frac{5}{4}}} \tag{64}$$

while for the u-quarks it is

$$T_u(p)=\pi T(f_2^2(p)-f_1^2(p))+2ipf_2(p)f_1(p) \tag{65}$$

with

$$f_1(p) \approx \frac{1}{3} f_2(p) \approx \frac{\omega_0}{(p^2 + (\nu_3 \omega_0)^2)^{\frac{5}{4}}}. \tag{66}$$

In the mean-field approximation, the modification of the effective pressure is

$$\begin{aligned} \mathcal{P}_{uds} - \mathcal{P}_{per} = & +24\pi (f_1 f_2 f_3 \nu_1 \nu_2 \nu_3 \Sigma_d^2 \Sigma_u)^{\frac{1}{3}} \\ & - 4\Sigma_d \Lambda_d - 2\Sigma_u \Lambda_u \\ & + \int \frac{d^3 p}{(2\pi)^3} \ln((1 + \Lambda_d^2 |T_d|^2)^2 \\ & \times (1 + \Lambda_u^2 |T_u|^2)) \end{aligned} \tag{67}$$

where $\mathcal{P}_{per}$ is the perturbative contribution with twisted quark boundary conditions [17]. For $\nu_1 \to 1/3$ the holonomy -induced masslike contribution in (64) becomes arbitrarily small. As we noted earlier, we use it to regulate the infrared sensitivity of the ds-contributions in (67) through a suitable redefinition of the fugacities $f_{2,3}$ as in [6]. With this in mind, the extrema of (67) with respect to Σ, Λ yield the respective gap equations

$$\begin{aligned} \Lambda_d &= 4\pi f (\nu_1 \nu_2 \nu_3)^{\frac{1}{3}} \left(\frac{\Sigma_u}{\Sigma_d} \right)^{\frac{1}{3}} \\ \Lambda_u &= 4\pi f (\nu_1 \nu_2 \nu_3)^{\frac{1}{3}} \left(\frac{\Sigma_d}{\Sigma_u} \right)^{\frac{2}{3}} \\ \Sigma_i &= \int \frac{d^3 p}{(2\pi)^3} \frac{\Lambda_i |T_i(p)|^2}{1 + \Lambda_i^2 |T_i(p)|^2}. \end{aligned} \tag{68}$$

Using (68) in (67) results in the shifted pressure at the saddle point

$$\begin{aligned} & \mathcal{P}_{uds} - \mathcal{P}_{per} \\ & = \int \frac{d^3 p}{(2\pi)^3} \ln \left[(1 + \Lambda_d^2 |T_d|^2)^2 (1 + \left(\frac{\tilde{\Lambda}_0^3}{\Lambda_d^2} \right)^2 |T_u|^2 \right] \end{aligned} \tag{69}$$

with $\tilde{\Lambda}_0 = 4\pi f (\nu_1 \nu_2 \nu_3)^{\frac{1}{3}}$. We note that the gap equation follows from $d\mathcal{P}/d\Lambda_d = 0$. The chiral condensates follow from standard arguments as

$$\begin{aligned} \langle \bar{d} d \rangle = \langle \bar{s} s \rangle &= 2\Lambda_d T \int \frac{d^3 p}{(2\pi)^3} \frac{F_1^2(p) + F_2^2(p)}{1 + \Lambda_d^2 |T_d(p)|^2} \\ \langle \bar{u} u \rangle &= 2\Lambda_u T \int \frac{d^3 p}{(2\pi)^3} \frac{f_1^2(p) + f_2^2(p)}{1 + \Lambda_u^2 |T_u(p)|^2}. \end{aligned} \tag{70}$$

In contrast and at asymptotically high temperatures, the $1/p^5$ contribution in the hopping matrix element (25) is dominant. Therefore the u-hopping is different from the d- and s-hoppings with $T_1(p) \approx 3T_2(p)$. The extrema of the pressure in $\Lambda_{1,2,3}$ are now found to be

$$3\Lambda_1 = \Lambda_2 = \Lambda_3 = \frac{4\pi T}{3} (3\nu_1 \nu_2 \nu_3 f_1 f_2 f_3)^{\frac{1}{3}} \tag{71}$$

with distinct chiral condensates

$$3\langle \bar{u} u \rangle \approx \langle \bar{d} d \rangle \approx \langle \bar{s} s \rangle \approx 0.78 T^3 (\tilde{\Lambda}_2)^{\frac{3}{5}}. \tag{72}$$

The high temperature phase breaks flavor symmetry but preserves the discrete combined charge conjugation symmetry and the exchange $d \leftrightarrow s$. As a check on these observations, we note that for $\tilde{\Lambda} \approx 1$, the chiral condensates in (61) are numerically close:

$$\begin{aligned} \langle \bar{q} q \rangle_{\tilde{\phi} = \pi} &\approx 0.61 T^3 \\ \langle \bar{q} q \rangle_{\tilde{\phi} = \frac{\pi}{3}} &\approx 0.76 T^3. \end{aligned} \tag{73}$$

The remaining task is to solve the gap equations for the four remaining parameters $\Lambda_d, \Lambda_u, \epsilon_1, \epsilon_2$. The numerical analysis of those equations will be presented elsewhere.

C. $N_c = N_f = 2$ in symmetric phase

The analysis of $N_f = N_c = 2$ follows similar arguments using the twisted boundary conditions (15) for $\pi\nu > \theta$. In this case the u-flavor rides the L-dyon, and the d-flavor rides the M-dyon with the hopping matrices

$$\begin{aligned} T_u(p) &= (\pi - \theta) T (\tilde{f}_2^2(p) - \tilde{f}_1^2(p)) + 2ip \tilde{f}_1(p) \tilde{f}_2(p) \\ T_d(p) &= \theta T (f_2(p)^2 - f_1^2(p)) + 2ip f_1(p) f_2(p) \end{aligned} \tag{74}$$

with

$$f_1(p) \approx \frac{1}{3} f_2(p) \approx \frac{\omega_0}{(p^2 + ((\nu - \theta/\pi)\omega_0)^2)^{\frac{5}{4}}}. \tag{75}$$

$\tilde{f}_{1,2}$ follows from $f_{1,2}$ using the substitution $\theta \to -\pi + \theta$. We note that for $\theta = 0$, the first contribution in T_d vanishes, since the d-boundary is periodic with zero Matsubara frequency. It is proportional to the Matsubara frequency in T_u, since the u-boundary is antiperiodic. This difference is in addition to the different masslike contributions induced by the holonomy ($\nu\omega_0$ for d and $\tilde{\nu}\omega_0$ and for u), which regulate the small-momenta (large-distance) behavior of the hopping amplitudes and causes the flavor condensates to be relatively different.

In the mean-field limit, the nonperturbative pressure is

$$\begin{aligned} \mathcal{P}_{ud} - \mathcal{P}_{per} = & 16\pi f (\nu_1 \nu_2 \Sigma_1 \Sigma_2)^{\frac{1}{2}} - 2\Lambda_1 \Sigma_1 - 2\Lambda_2 \Sigma_2 \\ & + \sum_{i=1,2} \int \frac{d^3 p}{(2\pi)^3} \ln(1 + \Lambda_i^2 |T_i(p)|^2) \end{aligned} \tag{76}$$

while the perturbative one (with our twisted boundary conditions) is given by

$$\mathcal{P}_{per} = -\frac{4\pi^2 T^3}{3}(\nu_1\nu_2)^2 - \frac{4T^3}{\pi^2}\sum_f\sum_{n=1}^{\infty}\frac{(-1)^n e^{i\theta_f n}}{n^4}\mathrm{Tr}_f L^n. \quad (77)$$

The first contribution comes from the gluons, while the second contribution comes from the twisted quarks. The Polyakov line L is in the fundamental representation, with the flavor twist explicitly factored out. The dominant contribution in the sum stems from the $n=1$ term. Note that for $\theta_1 = 0$ and $\theta_2 = \pi$, the fermionic contribution almost cancels.

The gap equations related to the parameters Λ_i, Σ_i are

$$\Lambda_1 = 4\pi f(\nu_1\nu_2)^{\frac{1}{2}}\left(\frac{\Sigma_2}{\Sigma_1}\right)^{\frac{1}{2}}$$
$$\Lambda_2 = 4\pi f(\nu_1\nu_2)^{\frac{1}{2}}\left(\frac{\Sigma_1}{\Sigma_2}\right)^{\frac{1}{2}}$$
$$\Sigma_i = \int\frac{d^3p}{(2\pi)^3}\frac{\Lambda_i|T_i|^2}{1+\Lambda_i^2|T_i(p)|^2}. \quad (78)$$

The chiral condensates are readily obtained as

$$\langle\overline{q}_i q_i\rangle = 2\Lambda_i T\int\frac{d^3p}{(2\pi)^3}\frac{f_1^2(p)+f_2^2(p)}{1+\Lambda_i^2|T_i(p)|^2}. \quad (79)$$

We note that for large Λ or asymptotically small temperatures, the second term in (30) proportional to p is dominant. In this case, the hopping matrix elements for M, L are equal. It follows that the extrema of the pressure (76) are also equal,

$$\Lambda \equiv \Lambda_1 = \Lambda_2 = 2\pi(f_L f_M)^{\frac{1}{2}}. \quad (80)$$

In this limit, the chiral condensates are also the same:

$$\langle\overline{u}u\rangle \approx \langle\overline{d}d\rangle \approx 2\Lambda T\int\frac{d^3p}{(2\pi)^3}\frac{f_1^2(p)+f_2^2(p)}{1+\Lambda^2|T_{1,2}(p)|^2} \quad (81)$$

with $f_{1,2}(p)$ given in (29).

Before we discuss the general asymmetric case, let us make the following comments on the so-called Roberge-Weiss symmetry [17]. Since the hopping matrix elements satisfy the antiperiodicity condition (31), the pressure (76) satisfies the so-called *half*-periodicity condition

$$\mathcal{P}(\theta+\pi/2) = \mathcal{P}(\theta-\pi/2) \quad (82)$$

in the center symmetric phase. Using the explicit form (30), we find that

$$\left(\frac{d\mathcal{P}}{d\theta}\right)_{\theta\to\pi/2} = 0 \quad (83)$$

which is cusp free despite the switching of the zero mode from the M- to the L-instanton-dyon. These observations are in agreement with those put forth by Roberge and Weiss [17] at low temperatures. At high temperature (83) develops a cusp in the center asymmetric phase [17]. We have checked that these properties hold also for the twisted boundary condition (15).

D. $N_c = N_f = 2$: General asymmetric case

To proceed, we first note that the gap equations (78) can be simplified by noting that $\Lambda_1\Lambda_2 = n^2$ and that $\Lambda_2\Sigma_2 = \Lambda_1\Sigma_1$. We have set $n = 4\pi f(\nu_1\nu_2)^{\frac{1}{2}}$ with $\nu_1 = \nu$ and $\nu_2 = 1-\nu$. With this in mind, (78) reduces to a single gap equation,

$$\int d^3\tilde{p}\,\frac{|\tilde{T}_1|^2}{1/\tilde{\Lambda}_1^2+|\tilde{T}_1|^2} = \int d^3\tilde{p}\,\frac{|\tilde{T}_2|^2}{\tilde{\Lambda}_1^2/\tilde{n}^4+|\tilde{T}_2|^2}. \quad (84)$$

After rescaling of all variables $\tilde{p} = p/\omega_0$, $\tilde{\Lambda}_{1,2} = \Lambda_{1,2}/\omega_0^2$ and $\tilde{n} = n/\omega_0^2$ with $\omega_0 = \pi T$, the hopping matrices (74) simplify:

$$|\tilde{T}_1|^2 \approx \frac{(6\tilde{p})^2}{(\tilde{p}^2+\nu_1^2)^5}$$
$$|\tilde{T}_2|^2 \approx \frac{64+(6\tilde{p})^2}{(\tilde{p}^2+\nu_2^2)^5}. \quad (85)$$

After using the gap equations (78) and the rescaling, the pressure (76) becomes

$$\frac{\mathcal{P}_{ud}}{\omega_0^3} = \int\frac{d^3\tilde{p}}{(2\pi)^3}\ln\left[(1+\tilde{\Lambda}_1^2|\tilde{T}_1|^2)\left(1+\left(\frac{\tilde{n}^2}{\tilde{\Lambda}_1}\right)^2|\tilde{T}_2|^2\right)\right] - \frac{4\pi^2}{3}\frac{T^3}{\omega_0^3}(\nu_1\nu_2)^2. \quad (86)$$

Its extremum in Λ is the gap equation $\partial\mathcal{P}_{ud}/\partial\tilde{\Lambda}_1 = 0$, which is (84). Similarly, there is the gap equation for the holonomy ν. The task is to solve them together. We found that (86) leads to the momentum-dependent constituent masses for the d-, u-quarks:

$$\frac{M_d(p)}{\omega_0} \equiv (1+\tilde{p}^2)^{\frac{1}{2}}\tilde{\Lambda}_1|\tilde{T}_1(p)|$$
$$\frac{M_u(p)}{\omega_0} \equiv (1+\tilde{p}^2)^{\frac{1}{2}}\frac{\tilde{n}^2}{\tilde{\Lambda}_1}|\tilde{T}_2(p)|. \quad (87)$$

The u-quark is substantially heavier than the d-quark at low momentum because of its antiperiodic boundary condition,

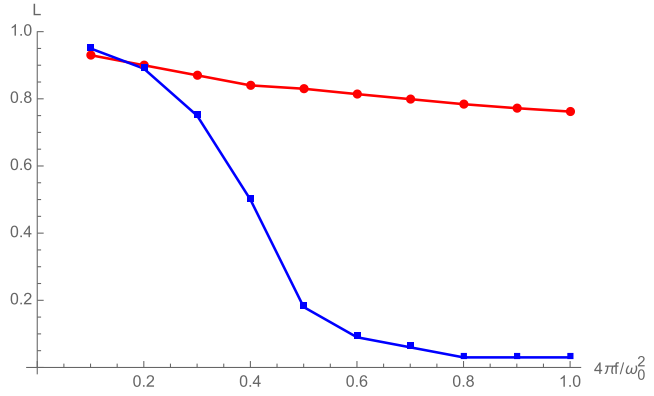

FIG. 1. Polyakov line versus the dimensionless density $\mathbf{n} = 4\pi f/\omega_0^2$ for $N_f = N_c = 2$. The lower line (blue squares) is for the Z_2 twisted quarks, while the upper line (red circles) is for the usual antiperiodic quarks.

with the d-quark turning massless at zero momentum owing to its periodic boundary condition.

The results for the numerical solution of the gap equations are shown in Figs. 1 and 2. In Fig. 1, we show the dependence of the Polyakov line $L = \cos(\pi\nu[\mathbf{n}])$ on the input parameter $\mathbf{n} = 4\pi f/\omega_0^2$ (blue squares) in the lower line. For comparison we also show the behavior of the same Polyakov line (red circles) in the upper line, for the untwisted (QCD) theory with both u- and d-quarks being antiperiodic fermions. The input parameter $\mathbf{n}$ is a definite monotonously decreasing function of the temperature as defined in (2). The rightmost part of the plot corresponds to the dense low-T case, in which we find a confining or $L \to 0$ behavior. The main conclusion from this plot is that confinement (or restoration of center symmetry) occurs at a lower density $\mathbf{n}$ for the twisted theory, as compared to the QCD-like one.

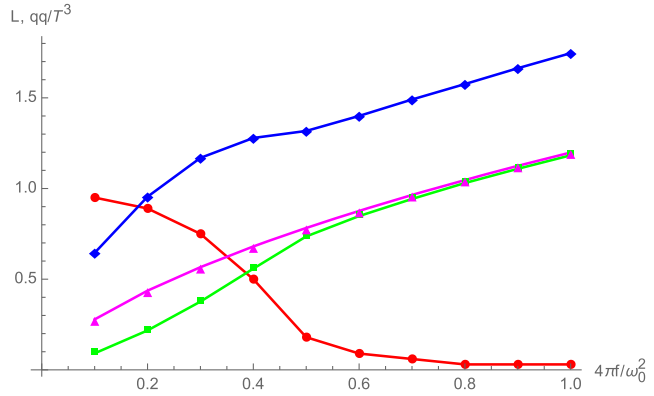

FIG. 2. Dimensionless condensates $|\langle\bar{d}d\rangle|/T^3$ (blue diamonds), $|\langle\bar{u}u\rangle|/T^3$ (green squares) for twisted boundary conditions, with increasing dimensionless density or lower temperatures $4\pi f/\omega_0^2$. For comparison we show $|\langle\bar{u}u\rangle|/T^3$ (magenta triangles) for the antiperiodic quarks. The Polyakov line (red squares) shows a rapid crossing from a center broken to a center symmetric phase for the twisted quarks.

In Fig. 2 we show the behavior of the flavor condensates $|\langle\bar{d}d\rangle|/T^3$ (blue diamonds), $|\langle\bar{u}u\rangle|/T^3$ (green squares) for the twisted u-, d-quarks versus $\mathbf{n} = 4\pi f/\omega_0^2$. For comparison, we also show the value of $|\langle\bar{u}u\rangle|/T^3 = |\langle\bar{d}d\rangle|/T^3$ (magenta triangles) for the untwisted (antiperiodic) boundary conditions. It follows closely the line for the antiperiodic d-quark in the twisted case. The value of the Polyakov line for the twisted quarks is shown also (red circles), to indicate the transition region. At moderately high densities or low temperatures, center symmetry is restored but the quark condensates are still distinct for the twisted boundary condition. The induced effective masses in (87) show that the d-quark is much lighter than the u-quark, resulting in a much larger chiral condensate. Only at vanishingly small temperatures, the relation (81) is recovered as both hoppings become identical. The nature of the boundary condition becomes irrelevant at zero temperature. However, as the temperature decreases the truncation of our analysis of the zero modes to their lowest Matsubara frequencies is no longer valid, as higher mode contributions become significant. As noted earlier in Sec. II C, the results in Fig. 2 for the various condensates cannot be extrapolated reliably to zero temperature or very high densities. At low densities or high temperatures, center symmetry is broken and the chiral condensate $|\langle\bar{d}d\rangle|$ is still substantially larger than $|\langle\bar{u}u\rangle|$.

E. Comparison to simulations

Our mean-field results are in qualitative but not quantitative agreement with recent simulations carried out in [22]. In particular, we found that $N_c = N_f = 2$ Z_2 twisted QCD has two distinct phases, the center symmetric and center asymmetric ones. However, the simulation in [22] observes a significant jump in the Polyakov line, concluding that the deconfinement transition is first order. Our numerical mean-field solutions of the gap equations as shown in (1)–(2) do not find a jump. They suggest that the transition is perhaps second order.

We find that the chiral condensates $\bar{u}u$ and $\bar{d}d$ are different from each other in both phases. In the asymmetric phase this result is in agreement with the one obtained in [22]. However, this agreement does not carry to the symmetric phase where in [22] the chiral condensates appear to be the same within error bars. Also, in our mean-field analysis, the smallest of the condensates induced by the L-dyons in twisted Z_2 QCD and ordinary QCD are very close. In [22] both condensates are found to be much larger than in ordinary QCD. In agreement with [22], we observe that in the interval of densities studied none of the chiral condensates vanishes. Both results see no chiral restoration transitions in Z_2 QCD.

Unfortunately, a qualitative comparison between our analysis and that of [22] is not yet possible. One reason for this is that in [22] the simulations were carried out using a simplified hopping matrix element (in coordinate

representation) for numerical convenience, as opposed to the one derived above directly from the exact zero modes. But even if all the settings were made identical, the agreement perhaps could only be expected in the very dense regime. As the ensemble of dyons and antidyons becomes dilute, clustering is expected with a breakdown of the mean-field assumption. This behavior is better studied using numerical simulations, where one can easily enforce randomization of the positions of the instanton-dyons.

F. Mesonic spectrum

The excitation spectrum with twisted boundary conditions can be calculated following the analysis in [4]. For the $N_c = N_f = 2$ case, this follows by substituting

$$\Lambda(\psi^\dagger\gamma_\pm\psi + 2\Sigma^\pm) \to \sum_{fg}\Lambda^\pm_{fg}(\psi^\dagger_f\gamma_\pm\psi_g + 2\Sigma^\pm_{fg}) \tag{88}$$

in (55) with

$$\Lambda_\pm \equiv \Lambda_0 \pm i\pi_{ps} + \pi_s = \mathrm{diag}(\Lambda_1,\Lambda_2) \pm i\pi_{ps} + \pi_s. \tag{89}$$

Here $\pi_{s,ps}$ refer to the scalar and pseudoscalar $U(2)$-valued mesonic fields.

For the chargeless chiral partners σ^3, π^0, the effective actions to quadratic order are respectively given by

$$\begin{aligned} S(\pi^3_{ps}) &= \frac{1}{2f_\pi^2}\int\frac{d^3p}{(2\pi)^3}\pi^3_{ps}(p)\Delta^3_-(p)\pi^3_{ps}(-p)\\ S(\pi^3_s) &= \frac{1}{2f_\pi^2}\int\frac{d^3p}{(2\pi)^3}\pi^3_s(p)\Delta^3_+(p)\pi^3_s(-p) \end{aligned} \tag{90}$$

with the corresponding propagators ($p_\pm = q \pm p/2$)

$$\begin{aligned} \Delta^3_\pm(p) = &\frac{1}{2}\int\frac{d^3q}{(2\pi)^3}\frac{(T_1(p_+)\pm T_1(p_-))^2}{(1+\Lambda_1^2|T_1(p_+)|^2)(1+\Lambda_1^2|T_1(p_-)|^2)}\\ &+\frac{1}{2}\int\frac{d^3q}{(2\pi)^3}\frac{(T_2(p_+)\pm T_2(p_-))^2}{(1+\Lambda_2^2|T_2(p_+)|^2)(1+\Lambda_2^2|T_2(p_-)|^2)} \end{aligned} \tag{91}$$

with the hopping matrices $T_{1,2}$ labeled as $1 \equiv d$ and $2 \equiv u$. In deriving (90)–(91) we made explicit use of the gap equations (78). We note that $\Delta^3_-(0) = 0$ translates to a massless $\pi^0 = \pi^3_{ps}$, while $\Delta^3_+(0) \neq 0$ translates to a massive σ, for both the center symmetric and broken phases. The masslessness of π^0 is ensured by the hidden symmetry displayed in (48)–(49), and reflects on the remaining spontaneously broken symmetry for $N_f = 2$.

The charged mesons $\pi^\pm_s, \pi^\pm_{ps}$ follow a similar analysis with now the propagators for the quadratic contributions given by

$$\Delta^{1,2}_\pm(p) = \frac{(\Sigma_1\Sigma_2)^{\frac{1}{2}}}{\pi f} - 2\int\frac{d^3q}{(2\pi)^3}\mathbb{F}_\mp(p,q). \tag{92}$$

Here $\Delta^{1,2}_-$ refer to the charged scalars $\pi^\pm_s$, while $\Delta^{1,2}_+$ refer to their charged chiral partners $\pi^\pm_{ps}$, with

$$\mathbb{F}_\pm(p,q) = \frac{T_1(p_+)T_2(p_-)(\Lambda_1\Lambda_2T_1(p_+)T_2(p_-)\pm 1)}{(1+\Lambda_1^2|T_1(p_+)|^2)(1+\Lambda_2^2|T_2(p_-)|^2)}. \tag{93}$$

In the exactly center symmetric phase, with $\Lambda_1 = \Lambda_2$, the charged pions $\pi^\pm_{ps}$ are also massless. But in general, in the asymmetric phase $\Lambda_1 \neq \Lambda_2$, and both $\pi^\pm$ are massive (but degenerate).

The singlet meson $\sigma = \pi_{s0}, \eta = \pi_{ps,0}$ propagators follow similarly:

$$\begin{aligned} 2\Delta_\sigma(p) &= \frac{n_D}{2} + \Delta^3_+(p)\\ 2\Delta_\eta(p) &= \frac{n_D}{2} + \Delta^3_-(p) \end{aligned} \tag{94}$$

with n_D the mean instanton-dyon density defined through the gap equation

$$\frac{n_D}{4} = \frac{1}{2}\sum_{i=1}^{2}\int\frac{d^3p}{(2\pi)^3}\frac{\Lambda_i^2|T_i|^2}{1+\Lambda_i^2|T_i|^2}. \tag{95}$$

V. CONCLUSIONS

We have constructed the partition function for the instanton-dyon liquid model with twisted flavor boundary conditions, and derived and solved the resulting gap equations in the mean-field approximation. In addition to manifest $U^{N_F}(1)\times U^{N_f}(1))/U_{L-R}(1)$ flavor symmetries, for Z_{N_c}-QCD some discrete charge conjugation plus flavor exchange symmetries were identified.

The central constructs are the so-called hopping matrix elements between instanton-dyon and anti-instanton-dyon zero modes. One technical point is to note that some of these hoppings may become singular at large distances (small momenta) when the contribution from the Z_{N_c}-twists and the holonomies cancel the exponentially decreasing asymptotics. These singularities are readily regulated through a suitable redefinition of the pertinent fugacities [6].

The low temperature phase is center symmetric with zero Polyakov line. It also breaks chiral symmetry, with still sizably different chiral condensates in our mean-field analysis. The latter are about equal at very small temperatures. The high temperature phase is center asymmetric with always unequal chiral condensates. Our results are qualitatively consistent with the lattice results reported recently in [20], although with a more pronounced difference between the flavor chiral condensates across the

transition region caused mostly by the differences in the leading (twisted) Matsubara modes in the center symmetric phase. In the symmetric ground state we observe the emergence of one massless pion π^0 (two-flavor case).

The instanton-dyon model offers a very concise framework for discussing the interplay of twisted boundary conditions (also known as flavor holonomies) with center symmetry and chiral symmetry in the QCD-like models. A further comparison between the mean-field results derived in this paper, with the direct simulations [22] of the instanton-dyon model and lattice results [20], is obviously of great interest.

ACKNOWLEDGMENTS

We thank Takumi Iritani for an early discussion. This work was supported by the U.S. Department of Energy under Contract No. DE-FG-88ER40388.

[1] R. A. Soltz, C. DeTar, F. Karsch, S. Mukherjee, and P. Vranas, Lattice QCD thermodynamics with physical quark masses, Annu. Rev. Nucl. Part. Sci. **65**, 379 (2015).

[2] V. G. Bornyakov, E.-M. Ilgenfritz, B. V. Martemyanov, and M. Muller-Preussker, Dyon structures in the deconfinement phase of lattice gluodynamics: Topological clusters, holonomies and Abelian monopoles, Phys. Rev. D **91**, 074505 (2015); Dyons near the transition temperature in lattice QCD, Phys. Rev. D **93**, 074508 (2016).

[3] Y. Liu, E. Shuryak, and I. Zahed, Confining dyon-antidyon Coulomb liquid model. I., Phys. Rev. D **92**, 085006 (2015).

[4] Y. Liu, E. Shuryak, and I. Zahed, Light quarks in the screened dyon-antidyon Coulomb liquid model. II., Phys. Rev. D **92**, 085007 (2015).

[5] Y. Liu, E. Shuryak, and I. Zahed, The instanton-dyon liquid model III. Finite Chemical Potential, arXiv:1606.07009.

[6] Y. Liu, E. Shuryak, and I. Zahed, Light adjoint quarks in the instanton-dyon liquid model IV, arXiv:1605.07584 (to be published).

[7] T. C. Kraan and P. van Baal, Periodic instantons with nontrivial holonomy, Nucl. Phys. **B533**, 627 (1998); Monopole constituents inside SU(n) calorons, Phys. Lett. B **435**, 389 (1998); K. M. Lee and C. h. Lu, SU(2) calorons and magnetic monopoles, Phys. Rev. D **58**, 025011 (1998).

[8] D. Diakonov and V. Petrov, Confining ensemble of dyons, Phys. Rev. D **76**, 056001 (2007); Confining ensemble of dyons, Phys. Rev. D **76**, 056001 (2007); Confinement and deconfinement for any gauge group from dyons viewpoint, AIP Conf. Proc. **1343**, 69 (2011); D. Diakonov, How to check that dyons are at work?, arXiv:1012.2296.

[9] D. Diakonov, N. Gromov, V. Petrov, and S. Slizovskiy, Quantum weights of dyons and of instantons with nontrivial holonomy, Phys. Rev. D **70**, 036003 (2004).

[10] R. Larsen and E. Shuryak, Classical interactions of the instanton-dyons with antidyons, Nucl. Phys. **A950**, 110 (2016).

[11] A. R. Zhitnitsky, Confinement-deconfinement phase transition and fractional instanton quarks in dense matter, arXiv:hep-ph/0601057; S. Jaimungal and A. R. Zhitnitsky, Monopoles and Coulomb gas representation of the QCD effective Lagrangian, arXiv:hep-ph/9905540; A. Parnachev and A. R. Zhitnitsky, Phase transitions, theta behavior and instantons in QCD and its holographic model, Phys. Rev. D **78**, 125002 (2008); A. R. Zhitnitsky, Conformal window in QCD for large numbers of colors and flavors, Nucl. Phys. **A921**, 1 (2014).

[12] M. Unsal and L. G. Yaffe, Center-stabilized Yang-Mills theory: Confinement and large N volume independence, Phys. Rev. D **78**, 065035 (2008); M. Unsal, Magnetic bion condensation: A new mechanism of confinement and mass gap in four dimensions, Phys. Rev. D **80**, 065001 (2009); E. Poppitz, T. Schafer, and M. Unsal, Continuity, deconfinement, and (super) Yang-Mills theory, J. High Energy Phys. 10 (2012) 115; E. Poppitz and M. Unsal, Seiberg-Witten and "Polyakov-like" magnetic bion confinements are continuously connected, J. High Energy Phys. 07 (2011) 082; E. Poppitz, T. Schafer, and M. Unsal, Universal mechanism of (semi-classical) deconfinement and theta-dependence for all simple groups, J. High Energy Phys. 03 (2013) 087.

[13] M. N. Chernodub, T. C. Kraan, and P. van Baal, Exact fermion zero mode for the new calorons, Nucl. Phys. B, Proc. Suppl. **83–84**, 556 (2000).

[14] E. Shuryak and T. Sulejmanpasic, The chiral symmetry breaking/restoration in dyonic vacuum, Phys. Rev. D **86**, 036001 (2012); Holonomy potential and confinement from a simple model of the gauge topology, Phys. Lett. B **726**, 257 (2013).

[15] P. Faccioli and E. Shuryak, QCD topology at finite temperature: Statistical mechanics of self-dual dyons, Phys. Rev. D **87**, 074009 (2013).

[16] E. Poppitz and T. Sulejmanpasic, (S)QCD on $\mathbb{R}^3 \times \mathbb{S}^1$: Screening of Polyakov loop by fundamental quarks and the demise of semi-classics, J. High Energy Phys. 09 (2013) 128.

[17] A. Roberge and N. Weiss, Gauge theories with imaginary chemical potential and the phases of QCD, Nucl. Phys. **B275**, 734 (1986).

[18] R. A. Janik, M. A. Nowak, G. Papp, and I. Zahed, Chiral disorder in two color QCD with Abelian external fluxes, Nucl. Phys. B, Proc. Suppl. **83–84**, 977 (2000); Two color QCD and Aharonov-Bohm fluxes, arXiv:hep-ph/9807499.

[19] H. Kouno, Y. Sakai, T. Makiyama, K. Tokunaga, T. Sasaki, and M. Yahiro, A QCD-like theory with the ZNc symmetry, arXiv:1202.5584; M. Yahiro, H. Kouno, Y. Sakai, T. Sasaki, and T. Makiyama, A simple model with Z_N symmetry, *Proc. Sci.*, LATTICE 2012 (2012) 099 [arXiv:1210.7567];

H. Kouno, T. Makiyama, T. Sasaki, Y. Sakai, and M. Yahiro, Confinement and $\mathbb{Z}_3$ symmetry in three-flavor QCD, J. Phys. G **40**, 095003 (2013).

[20] T. Iritani, E. Itou, and T. Misumi, Lattice study on QCD-like theory with exact center symmetry, J. High Energy Phys. 11 (2015) 159.

[21] A. Cherman, T. Schaefer, and M. Unsal, Chiral Lagrangian from Duality and Monopole Operators in Compactified QCD, Phys. Rev. Lett. **117**, 081601 (2016).

[22] R. Larsen and E. Shuryak, Instanton-dyon ensembles III: Exotic quark flavors, arXiv:1605.07474.

[23] T. Schafer and E. V. Shuryak, Instantons in QCD, Rev. Mod. Phys. **70**, 323 (1998); D. Diakonov, Instantons at work, Prog. Part. Nucl. Phys. **51**, 173 (2003); M. A. Nowak, M. Rho, and I. Zahed, *Chiral Nuclear Dynamics* (World Scientific, Singapore, 1996), p. 528.

[24] T. M. W. Nye and M. A. Singer, An L^2 index theorem for Dirac operators on $S^1 \times \mathbb{R}^3$, arXiv:math/0009144.

[25] A. M. Polyakov, Quark confinement and topology of gauge groups, Nucl. Phys. **B120**, 429 (1977).

[26] M. Kacir, M. Prakash, and I. Zahed, Hadrons and QCD instantons: A bosonized view, Acta Phys. Pol. B **30**, 287 (1999).